Microbiology (2014), **160**, 2208–2214 DOI 10.1099/mic.0.080234-0

Sro7 and Sro77, the yeast homologues of the *Drosophila* lethal giant larvae (Lgl), regulate cell proliferation via the Rho1–Tor1 pathway

Liang-Chun Liou,[1] Qun Ren,[1] Qiuqiang Gao[2] and Zhaojie Zhang[1]

[1]Department of Zoology and Physiology, University of Wyoming, Laramie, WY 82071, USA

[2]State Key Laboratory of Bioreactor Engineering, East China University of Science and Technology, 130 Meilong Road, Shanghai 200237, PR China

Correspondence
Zhaojie Zhang
zzhang@uwyo.edu

Received 17 April 2014
Accepted 22 July 2014

Saccharomyces cerevisiae Sro7 and Sro77 are homologues of the *Drosophila* tumour suppressor lethal giant larvae (Lgl), which regulates cell polarity in *Drosophila* epithelial cells. Here, we showed that double mutation of *SRO7*/*SRO77* was defective in colony growth. The colony of the *SRO7*/*SRO77* double deletion was much smaller than the WT and appeared to be round with a smooth surface, compared with the WT. Analysis using transmission electron microscopy revealed multiple defects of the colony cells, including multiple budding, multiple nuclei, cell lysis and dead cells, suggesting that the double deletion caused defects in cell polarity and cell wall integrity (CWI). Overexpression of *RHO1*, one of the central regulators of cell polarity and CWI, fully recovered the *sro7*Δ/*sro77*Δ phenotype. We further demonstrated that *sro7*Δ/*sro77*Δ caused a decrease of the GTP-bound, active Rho1, which in turn caused an upregulation of *TOR1*. Deletion of *TOR1* in *sro7*Δ/*sro77*Δ (*sro7*Δ/*sro77*Δ/*tor1*Δ) recovered the cell growth and colony morphology, similar to WT. Our results suggested that the tumour suppressor homologue *SRO7*/*SRO77* regulated cell proliferation and yeast colony development via the Rho1–Tor1 pathway.

INTRODUCTION

Saccharomyces cerevisiae Sro7 and Sro77 are functional homologues, and are involved in docking and fusion of post-Golgi vesicles with plasma membrane. Double deletion of *SRO7*/*SRO77* induces a severe defect in exocytosis as evidenced by the accumulation of post-Golgi vesicles (Lehman *et al.*, 1999). Sro7 and Sro77 are homologues of the *Drosophila* tumour suppressor lethal giant larvae (Lgl), which regulates the cell polarity in epithelial cells (Bilder, 2004; Gibson & Perrimon, 2003; Hariharan & Bilder, 2006). Loss of Lgl results in defects of cell polarization and carcinoma (Agrawal *et al.*, 1995).

In *S. cerevisiae*, polarized cell growth is regulated primarily by Rho-like GTPases, including Cdc42 and the Rho proteins (Rho1–Rho5) (Madden & Snyder, 1998; Bi & Park, 2012). Defects of cell polarization can be categorized into four classes: secretory block, secretory mistargeting, endocytic block and cell wall synthesis block (Pruyne & Bretscher, 2000). Cdc42 functions in the organization of actin filaments and septin. It also helps vesicle delivery to the site of bud growth and helps bud site selection (Adamo *et al.*, 2001; Pruyne & Bretscher, 2000). Cdc42 mutation results in budding polarization loss and isotropic growth at multiple random sites on the cell membrane. Rho1, an essential gene for polarized growth (Levin, 2011), plays an important role in the reorganization of the actin cytoskeleton and cell wall synthesis during cytokinesis. Rho1 controls the localization of the exocyst and actin filament assembly towards the budding sites with Cdc42.

The fact that Sro7/Sro77 are homologues of the *Drosophila* Lgl suggests that Sro7/Sro77 might also be involved in regulation of cell polarity in yeast. Transmission electron microscopy (TEM) was used to further examine *sro7*Δ/*sro77*Δ colony cells, which have a more profound phenotype than those of liquid culture. We showed that in a 3 day colony, *sro7*Δ/*sro77*Δ cells displayed multiple defects, including cell lysis, multiple budding, multiple nuclei and cell death. Moreover, we identified that Sro7/Sro77 are upstream regulators of the small GTPase Rho1, which in turn regulates the *TOR1* complex that controls asymmetrical cell growth. Our study sheds light on a possible role of Sro7/Sro77 as a cancer repressor and its mechanism of repressing cell growth.

Abbreviations: CWI, cell wall integrity; HA, haemagglutinin; RT, reverse transcription; TEM, transmission electron microscopy; TOR, target of rapamycin.

METHODS

Yeast strains and culture conditions. Yeast cells were grown on YPD plates (1 % yeast extract, 2 % peptone, 2 % glucose and 1.7 %

agar) at 30 °C or as otherwise noted in the text. The WT *S. cerevisiae* strain BY4742 (*Matα his3Δ leu2Δ met15Δ ura3Δ*) was purchased from Thermo Scientific. All other strains were derived from BY4742. Deletion of *SRO7* was introduced by the standard PCR-mediated gene replacement method (Wach *et al.*, 1994). For *SRO7*/*SRO77* double deletion, *SRO7* was deleted from the *sro77Δ* single-deleted strain using *URA3* as a selection marker. The triple deletion of *sro7Δ*/*sro77Δ*/*tor1Δ* was constructed using the *sro7Δ*/*sro77Δ* double mutant. *RHO1* and *CDC42* overexpression plasmids were purchased from Thermo Scientific. The genes were cloned into vector p5472 carrying a *URA3* selectable marker and a yeast centromere (Ho *et al.*, 2009). The expression of each gene was driven by its endogenous promoter and its normal 3′ untranslated region. The C-terminal Rho1-haemagglutinin (HA) tag was generated as previously described (Janke *et al.*, 2004).

TEM. Cells were cultured at 30 °C on YPD plates. Colonies were covered with a thin layer of 1 % low-melting-point agarose at 37 °C. The colony was then cut from the plate into small cubes, and fixed with 2 % glutaraldehyde and 2.5 % paraformaldehyde in 0.1 M cacodylic acid at room temperature overnight. The cubes were washed in the following order: 0.1 M cacodylic buffer (five times; 10 min each), deionized water (three times; 15 min each), 2 % sodium metaperiodate (one time; 50 min) and deionized water (two times; 15 min each). The cubes were then fixed in freshly prepared 2 % potassium permanganate overnight at room temperature. Fixed colonies were stained with 2 % uranyl acetate overnight at room temperature and dehydrated with serial ethanol [30, 50, 75, 85, 95 and 100 % (three times), each for 30–40 min]. Cells were transitioned with propylene oxide, infiltrated in EMBed 812 resin (Electron Microscopy Sciences). Ultrathin sections (50 nm) were cut and stained with lead citrate. Sections were examined using a Hitachi H-7000 electron microscope, equipped with a high-resolution (4K × 4K) digital camera (Gatan). The sections were imaged at × 1000 and the images were stitched together manually with Adobe Photoshop software.

Fluorescence microscopy. Cells were fixed with 4 % paraformaldehyde for 20 min. For visualization of chitin, cells were stained with 25 μM Fluorescent Brightener 28 (Sigma-Aldrich) in PBS (pH 7.4) for 30 min in the dark. For visualization of nuclei, cells were stained with DAPI (0.5 mg ml^{-1}). All images were taken using a Zeiss 710 laser scanning confocal microscope.

Semiquantitative reverse transcription (RT)-PCR. Total RNA from yeast cells was extracted using the RNeasy Protect Mini kit (Qiagen). The RT-PCR and the amplification procedure were performed as described previously (Gao *et al.*, 2009). The yeast actin gene (*ACT1*) was used as control, and the primers were 5′-TGTCACCAACTGGGACGATA-3′ and 5′-AACCAGCGTAAATTGGAACG-3′. Primers used for *RHO1* amplification were 5′-ACAAGAAAAATGGATTGCCG-3′ and 5′-ACGGGTTGTTGACCTTCTTG-3′. *TOR1* primers were 5′-CGTGAGCGTTACACTCGGTA-3′ and 5′-ATATCCCACTCTCCCAACCC-3′. *TOR2* primers were 5′-GCAAAGAATTCTGCGTGTCA-3′ and 5′-GCATAAACAACTGGAGGGGA-3′.

Western blot analysis. Cells were cultured at 30 °C in YPD to early exponential phase. Cell lysate preparation was according to Ren *et al.* (2012). Equivalent amounts of protein were separated by 10 % SDS-PAGE and transferred to PVDF membranes. The membranes were blocked in 5 % BSA for non-specific binding. The membranes were then incubated with rat anti-HA (1 : 1000 dilution; Roche Diagnostics) or rat anti-tubulin (1 : 2000 dilution; Abcam) as a loading control. The membrane was washed with blocking buffer, followed by goat anti-rat IgG conjugated with horseradish peroxidase (Thermo Scientific). Immunoreactive bands were visualized using a ChemiDoc system (Bio-Rad).

Rho1 pull-down assay. The active Rho1 (Rho1-GTP) was measured by using the Rho1-GTP pull-down kit (Cytoskeleton). Proteins were prepared in the same way as for Western blot analysis and normalized with the Bradford assay (Bradford, 1976). Normalized proteins were incubated with GTP-γS for 15 min as a positive control. Equal amounts of proteins were incubated with Rhotekin-RBD beads (Cytoskeleton) for 1 h at 4 °C. Pelleted beads were washed with washing buffer and the Rho1-GTP bound to beads was eluted with 2 × Laemmli buffer and boiled for 2 min. The eluted Rho1-GTP protein was analysed by Western blotting using anti-HA antibody.

Spot assays. Cells were cultured in YPD liquid medium overnight. Cells were harvested by centrifugation, washed once with water and then suspended in water. The cell concentration was 1×10^7 cells ml^{-1}. A fivefold serial dilution of these cells was made, and 4 μl of each dilution was spotted onto appropriate YPD and YPG (1% yeast extract, 2% peptone, 2% galactose) solid medium.

RESULTS

Double deletion of *SRO7* and *SRO77* (*sro7Δ*/*sro77Δ*) causes defects of colony development

It has been reported that the double deletion of *SRO7* and *SRO77* (*sro7Δ*/*sro77Δ*) is cold sensitive and has a defect in exocytosis (Lehman *et al.*, 1999). The *sro7Δ*/*sro77Δ* double deletion appeared to grow normally at 30 or 37 °C, but grew poorly at 24 °C. Overexpression of *SRO7* (*sro7Δ*/*sro77Δ* + *SRO7*) or *SRO77* (*sro7Δ*/*sro77Δ* + *SRO77*) recovered the growth defect of the *sro7Δ*/*sro77Δ* double deletion (Fig. 1a). *sro7Δ*/*sro77Δ* also affected colony growth, possibly due to its defect in exocytosis. As shown in Fig. 1(b), even at 30 °C, the *sro7Δ*/*sro77Δ* colony was much smaller than the WT. The colony appeared to be round with a smooth surface, compared with the WT, suggesting that the double deletion was defective in colony differentiation. To better understand its phenotype, we examined the internal structure of *sro7Δ*/*sro77Δ* colony cells using TEM. When grown on YPD for 3 days, the WT showed a normal cellular structure (Fig. 2a, b). In contrast, many dead cells were observed inside the *sro7Δ*/*sro77Δ* colony, especially near the middle part of the colony (Fig. 2c–g). One possibility was that the dead cells were older cells and they died to release nutrients to support the growth of the other cells (Váchová & Palková, 2005).

RHO1 overexpression recovers the *sro7Δ*/*sro77Δ* phenotype

TEM analysis revealed that some colony cells underwent cell lysis (Fig. 2f), suggesting a defect in the cell wall integrity (CWI) in the *sro7Δ*/*sro77Δ* mutant (Levin & Bartlett-Heubusch, 1992). Multiple nuclei and multiple buds were also observed in *sro7Δ*/*sro77Δ* colony cells (Fig. 2g, h), suggesting that the double deletion was defective in polarized cell growth. Staining with Fluorescent Brightener 28 showed that chitin was concentrated mainly on the bud scars in WT, but in *sro7Δ*/*sro77Δ* the chitin was spread across the cell wall (Fig. 3), further suggesting its defect in CWI. All these phenomena pointed to possible mis-regulation of small GTPases, *RHO1* and/or *CDC42*, the

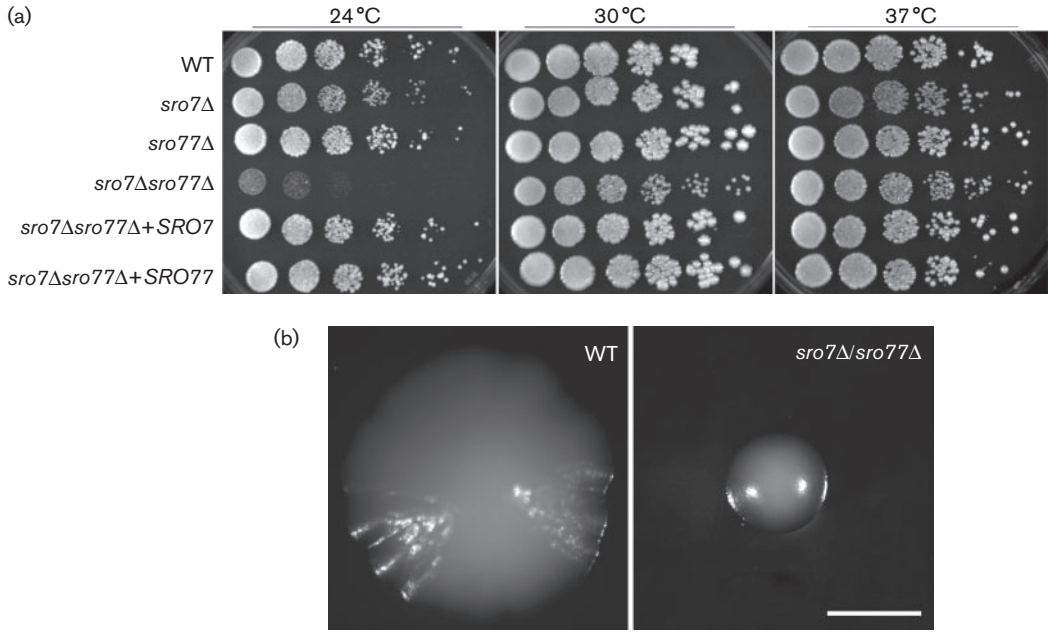

Fig. 1. Double deletion of *SRO7* and *SRO77* caused a defect of colony growth. (a) Spot assay showing that *sro7*Δ/*sro77*Δ cells are cold sensitive. Aliquots of cells were spotted on YPD plates using 4 μl serial 1 : 5 dilutions. Cells were cultured for 2 days at 24, 30 or 37 °C. (b) Single-colony morphology of *sro7*Δ/*sro77*Δ, which was much smaller and round with a smooth surface, compared with WT. The colony was grown on YPD plates at 30 °C for 3 days. Bar, 1 mm.

central regulators of cell polarity and CWI. To test this possibility, we overexpressed *CDC42* or *RHO1* in *sro7*Δ/*sro77*Δ (*sro7*Δ/*sro77*Δ + *CDC42* or *sro7*Δ/*sro77*Δ + *RHO1*). Overexpression of *CDC42* showed no apparent effect on colony growth. Overexpression of *RHO1*, however, fully recovered the *sro7*Δ/*sro77*Δ phenotype (Fig. 4). The colony of *sro7*Δ/*sro77*Δ + *RHO1* was similar to WT and no multiple nuclei or multiple budding was observed. Overexpression of *RHO1* also recovered the chitin localization in *sro7*Δ/*sro77*Δ, whilst no apparent difference was observed when *CDC42* was overexpressed (Fig. 3).

Rho1-GTP level is lower in the *sro7*Δ/*sro77*Δ deletion

The fact that *RHO1* overexpression recovered the *sro7*Δ/*sro77*Δ phenotype suggested that the *RHO1* level may be lower in the *sro7*Δ/*sro77*Δ strain. RT-PCR was used to compare the *RHO1* levels between WT and *sro7*Δ/*sro77*Δ. As shown in Fig. 5(a), the *RHO1* mRNA levels of WT and *sro7*Δ/*sro77*Δ were similar. Western blot showed that the Rho1 proteins of WT and *sro7*Δ/*sro77*Δ were also similar (Fig. 5b). Rho1 is a small GTPase, which switches from its GTP-bound, active form to a GDP-bound, inactive form. To examine if *SRO7*/*SRO77* was involved in the activation of *RHO1*, a pull-down assay was performed and our results showed that GTP-bound Rho1 (Rho1-GTP) was much lower in the *sro7*Δ/*sro77*Δ deletion than in the WT (Fig. 5c, top panel). To further confirm this, we overexpressed *ROM2* and *TUS1*, the guanine nucleotide-exchange factors of Rho1 that activate Rho1 by catalysing the dissociation of GDP, allowing GTP to bind to Rho1. The *sro7*Δ/*sro77*Δ grew slightly better when *TUS1* was overexpressed, while *ROM2* significantly recovered the *sro7*Δ/*sro77*Δ growth defect (Fig. 5d). Overexpression of *ROM2* also partially recovered the Rho1-GTP level of *sro7*Δ/*sro77*Δ (Fig. 5c, middle panel), further suggesting that the lack of active Rho1, rather than the total amount of Rho1, was responsible for the *sro7*Δ/*sro77*Δ phenotype.

TOR (target of rapamycin) proteins are protein kinases that play a central role in cell metabolism and polarized growth. Recent studies have shown that TOR is a direct target of the small GTPase Rho1 (Yan *et al.*, 2012). We speculated that *SRO7*/*SRO77* might regulate cell polarity via the Rho1→TOR pathway. To test this possibility, we first measured the mRNA level of *TOR1* and *TOR2* in the *sro7*Δ/*sro77*Δ double deletion. Whilst no obvious change was observed for *TOR2* mRNA levels, the *TOR1* mRNA level was much higher in *sro7*Δ/*sro77*Δ than in WT (Fig. 6a). Overexpression of *RHO1* reduced the *TOR1* level of *sro7*Δ/*sro77*Δ to the WT level, indicating that the *TOR1* mRNA increase in *sro7*Δ/*sro77*Δ was a consequence of a decreased level of active Rho1 in this strain (Fig. 6b). The *sro7*Δ/*sro77*Δ double deletion was also more sensitive to rapamycin, further suggesting its higher *TOR1* level, and overexpression of *RHO1* in *sro7*Δ/*sro77*Δ partially recovered its sensitivity to rapamycin (Fig. 6c). Deletion of *TOR1* in the *sro7*Δ/*sro77*Δ background (*sro7*Δ/*sro77*Δ/*tor1*Δ) recovered the cell growth and colony morphology, similar to WT (Fig. 6d).

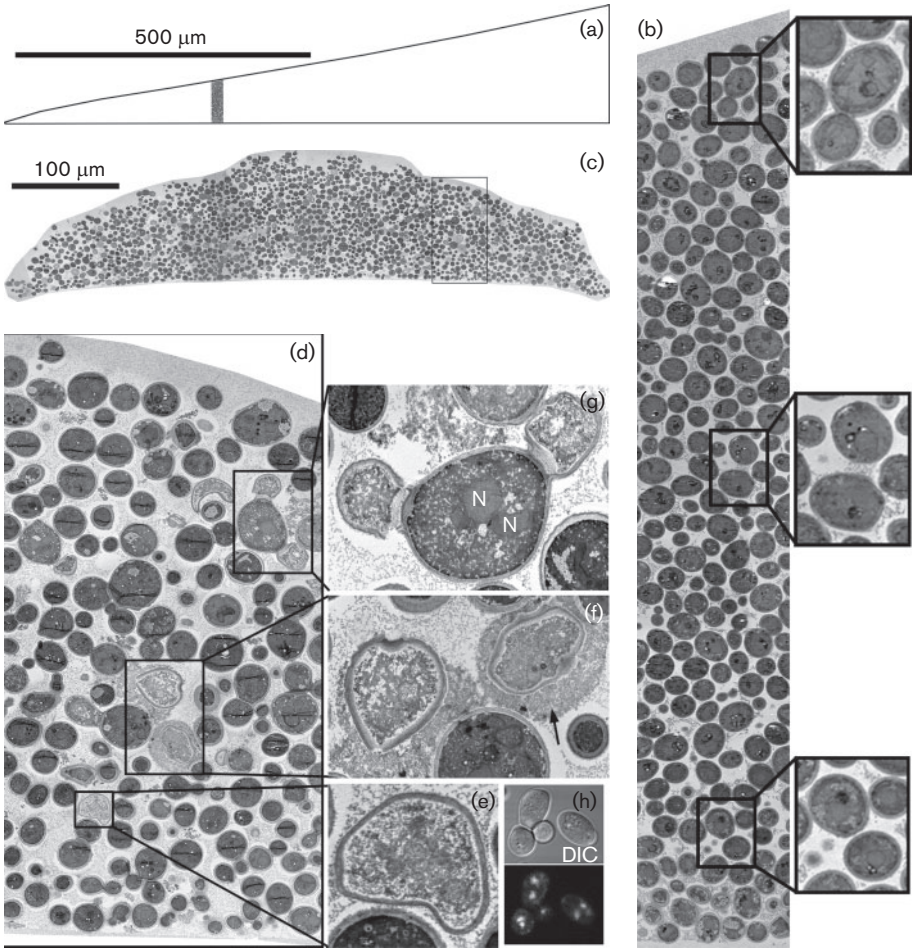

Fig. 2. Microscopy analysis of WT and *sro7*Δ/*sro77*Δ cells. (a, b). TEM cross-section of a WT, 3 day colony, showing normal structure of yeast cells in the colony. (a) Outline of a colony (half) grown on a YPD plate at 30 °C for 3 days. (b) TEM image of inset in (a). (c). TEM cross-section of a *sro7*Δ/*sro77*Δ colony on a YPD plate at 30 °C for 3 days. (d). TEM image of the boxed area in (c). (e–g). Cells at high magnification from (d), showing a dead cell (e), cell lysis (f), and multiple buds and multiple nuclei (g). Arrow in (f) indicates lysis of the cell wall. N, nucleus. (h) Confocal microscopy images showing multiple buds and multiple nuclei of *sro7*Δ/*sro77*Δ cells. DIC, differential interference contrast.

DISCUSSION

Sro7 and Sro77 were identified originally as high-copy suppressors of Rho3 mutants. They play important roles in the late stages of exocytosis (Lehman *et al.*, 1999). Consistent with previous studies (Lehman *et al.*, 1999; Zhang *et al.*, 2005), we observed that *sro7*Δ/*sro77*Δ displayed a multiple budding and multiple nuclei phenotype, which is more profound when grown on solid media than in liquid media. Cell lysis, which had been studied traditionally by examining the release of cellular material into the medium (Levin & Bartlett-Heubusch, 1992), was also observed in the *sro7*Δ/*sro77*Δ colony. Traditionally, when TEM is used to examine yeast cells, cells are fixed and processed in liquid, and therefore it is difficult to 'capture' the lysis process. The '*in situ*' fixation and process for TEM preparation enabled us to observe the cell lysis process directly. The phenomena of cell lysis (Fig. 2f) and the thickened, irregular cell wall between mother–daughter cells (Fig. 2g) strongly suggest that *sro7*Δ/*sro77*Δ is defective in the CWI pathway, which is regulated by the small GTPase Rho1 (Levin, 2005).

RHO1 is an essential gene and its main function is to regulate polarized growth and the organization of the actin cytoskeleton (Madden & Snyder, 1998). We demonstrated that overexpression of *RHO1* recovered the *sro7*Δ/*sro77*Δ phenotype, which is different from a previous report which showed that a high dose of *CDC42* or *RHO1* could not rescue the *sro7*Δ/*sro77*Δ phenotype (Zhang *et al.*, 2005). This difference is likely caused by different strain backgrounds. Overexpression of *ROM2*, a guanine nucleotide-exchange factor of Rho1, also recovered the *sro7*Δ/*sro77*Δ phenotype. In addition, the Rho1p-GTP level was

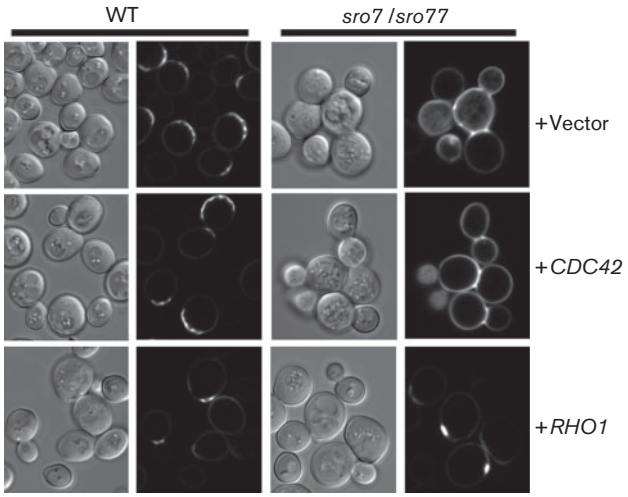

Fig. 3. Chitin staining of WT and *sro7*Δ/*sro77*Δ colony cells showing that chitin staining was localized mainly at the bud scars in WT, but across the cell wall in *sro7*Δ/*sro77*Δ (top panel). Overexpression of *CDC42* (+*CDC42*) had no effect on either WT or *sro7*Δ/*sro77*Δ (middle panel). Overexpression of *RHO1* (+*RHO1*) had no effect on WT, but recovered the phenotype of *sro7*Δ/*sro77*Δ (bottom panel).

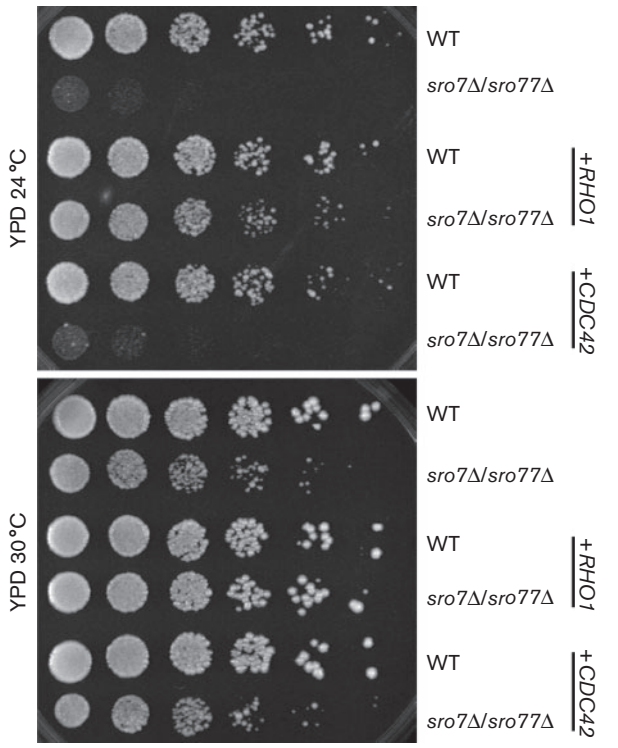

Fig. 4. Spot assay showing *RHO1* (+*RHO1*) overexpression in *sro7*Δ/*sro77*Δ recovered cell growth similar to WT. No apparent effect was seen for *CDC42* overexpression (+*CDC42*). Cells were cultured on YPD at 24 or 30 °C for 2 days.

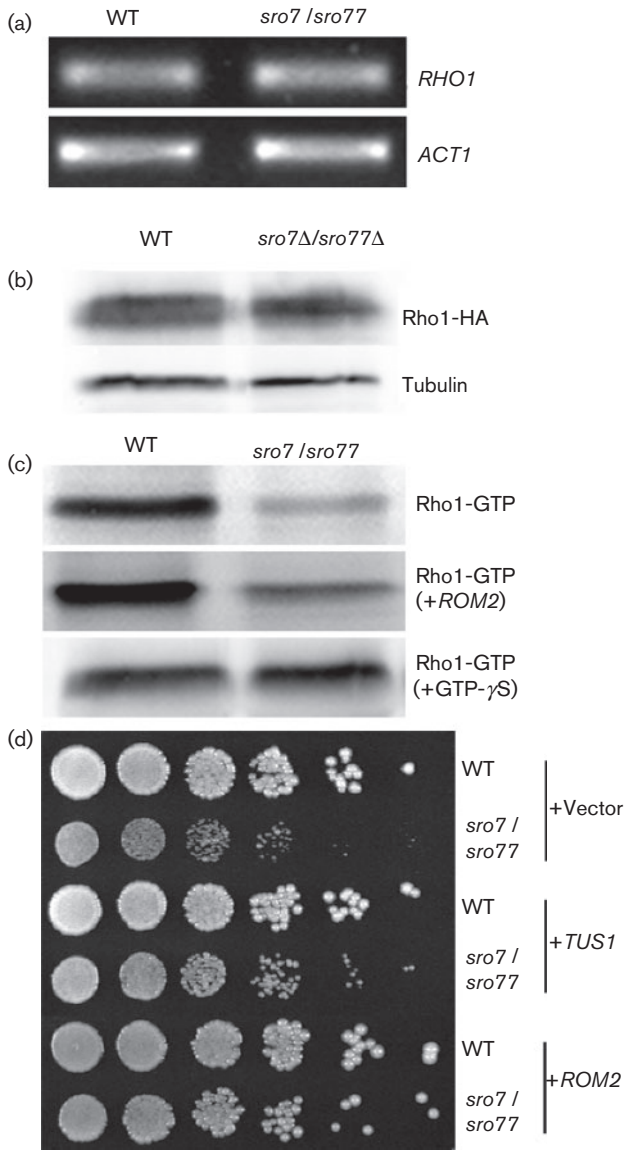

Fig. 5. *SRO7* and *SRO77* affected the level of Rho1-GTP. (a) RT-PCR analysis showing *RHO1* mRNA expression in *sro7*Δ/*sro77*Δ was similar to WT. *ACT1* was used as a control. (b) Western blot analysis showing the Rho1 protein level in *sro7*Δ/*sro77*Δ was similar to WT. Tubulin was used as a loading control. (c) Pull-down assay showing Rho1-GTP was decreased in *sro7*Δ/*sro77*Δ. Overexpression of *ROM2* increased the level of Rho1-GTP in both WT and *sro7*Δ/*sro77*Δ. GTP-γS was loaded as a positive control for total Rho1-GTP. (d) Spot assay showing *ROM2* overexpression recovered the growth defect of *sro7*Δ/*sro77*Δ, whilst the growth defect was only partially recovered when *TUS1* was overexpressed. Cells were cultured on YPD plates at 30 °C for 2 days.

much lower in the *sro7*Δ/*sro77*Δ strain and was restored partially when *ROM2* was overexpressed (Fig. 5c). These results indicate that *SRO7*/*SRO77* are upstream regulators for Rho1 activation. This notion is further supported by

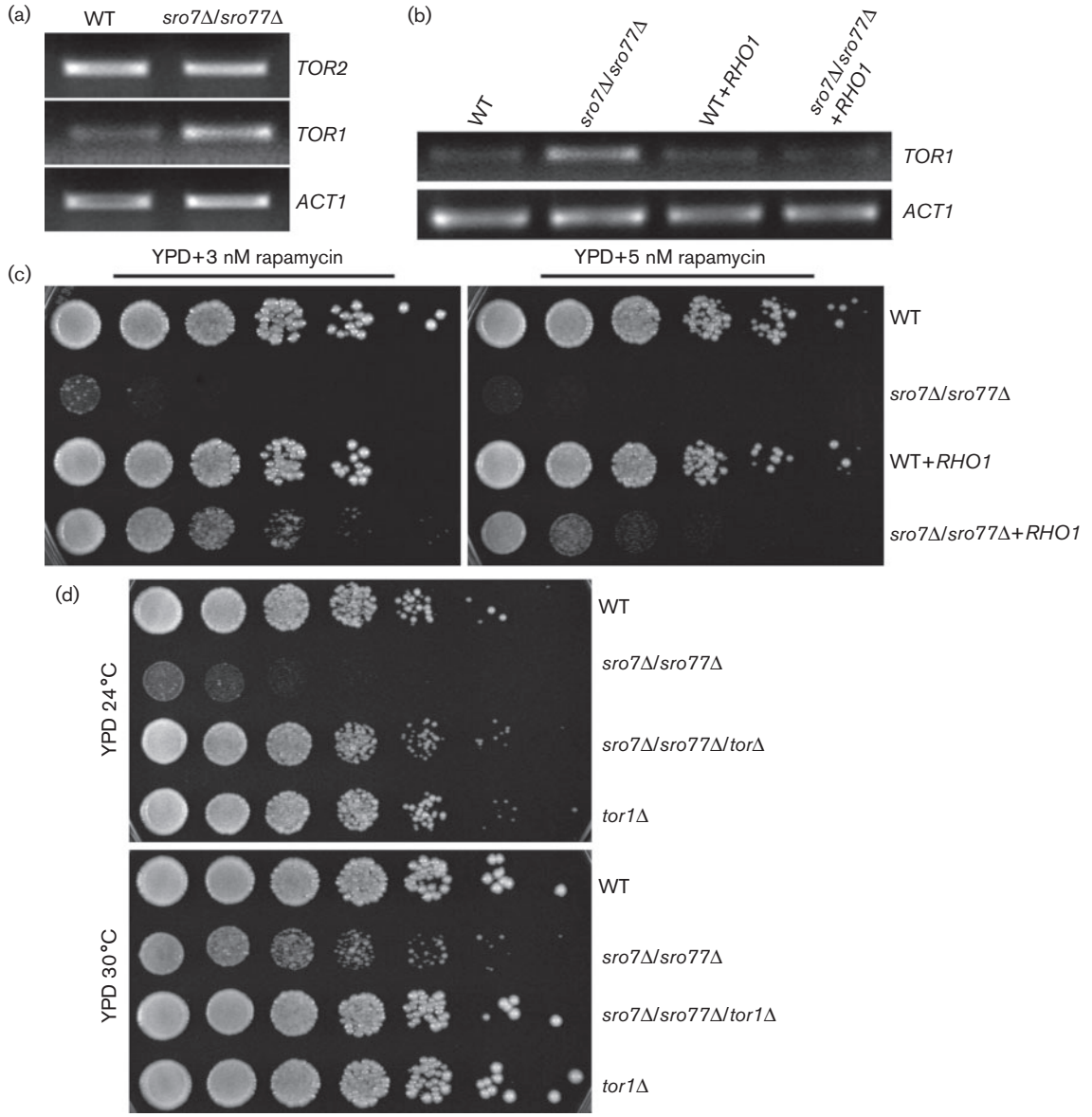

Fig. 6. *TOR1* mRNA was increased in *sro7*Δ/*sro77*Δ. (a) RT-PCR analysis showing *TOR1* mRNA was increased, whilst *TOR2* mRNA was unchanged in *sro7*Δ/*sro77*Δ. *ACT1* was used as a loading control. (b) RT-PCR analysis showing overexpression of *RHO1* reduced *TOR1* mRNA to the WT level. (c) Spot assay showing *sro7*Δ/*sro77*Δ was more sensitive to rapamycin compared with WT. *RHO1* overexpression partially recovered its sensitivity to rapamycin. Cells were cultured on YPD plates at 30 °C for 2 days. (d) Spot assay showing that the triple deletion *sro7*Δ/*sro77*Δ/*tor1*Δ recovered the growth defect of *sro7*Δ/*sro77*Δ at 24 and 30 °C on YPD for 2 days.

the fact that neither *RHO1* mRNA nor the Rho1 protein levels were decreased in *sro7*Δ/*sro77*Δ (Fig. 5a, b).

It has been reported recently (Yan *et al.*, 2012) that the Rho1 GTPase regulates directly the TOR complex 1 (TORC1) under stress conditions. Stresses, such as rapamycin or caffeine, induce the activation of Rho1, which in turn binds directly to and downregulates TORC1 activity. Consistent with these findings, we demonstrated that the lower level of the GTP-bound, active Rho1 in *sro7*Δ/*sro77*Δ caused an increased level of *TOR1*, which stimulates cell growth. Our results suggest strongly that Sro7/Sro77 may repress cell growth by regulating the *TOR1* pathway via the GTPase Rho1. The results also suggest that Sro7/Sro77 are upstream of the Rho1-regulated polarized cell growth (Fig. 7). These findings may shed light on the molecular mechanism of cell growth regulated by cancer repressors.

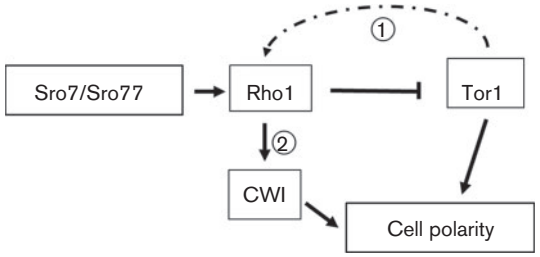

Fig. 7. Diagram of the possible pathway by which Sro7/Sro77 regulates cell polarity through Rho1 and Tor1. References: 1, Yan *et al.* (2012); 2, Levin (2005).

ACKNOWLEDGEMENTS

This study was supported in part by an Institutional Development Award from the National Institute of General Medical Sciences of the National Institutes of Health (grant P30 GM103398).

REFERENCES

Adamo, J. E., Moskow, J. J., Gladfelter, A. S., Viterbo, D., Lew, D. J. & Brennwald, P. J. (2001). Yeast Cdc42 functions at a late step in exocytosis, specifically during polarized growth of the emerging bud. *J Cell Biol* **155**, 581–592.

Agrawal, N., Kango, M., Mishra, A. & Sinha, P. (1995). Neoplastic transformation and aberrant cell–cell interactions in genetic mosaics of *lethal(2)giant larvae* (*lgl*), a tumor suppressor gene of *Drosophila*. *Dev Biol* **172**, 218–229.

Bi, E. & Park, H. O. (2012). Cell polarization and cytokinesis in budding yeast. *Genetics* **191**, 347–387.

Bilder, D. (2004). Epithelial polarity and proliferation control: links from the *Drosophila* neoplastic tumor suppressors. *Genes Dev* **18**, 1909–1925.

Bradford, M. M. (1976). A rapid and sensitive method for the quantitation of microgram quantities of protein utilizing the principle of protein-dye binding. *Anal Biochem* **72**, 248–254.

Gao, Q., Liu, Y., Wang, M., Zhang, J., Gai, Y., Zhu, C. & Guo, X. (2009). Molecular cloning and characterization of an inducible RNA-dependent RNA polymerase gene, GhRdRP, from cotton (*Gossypium hirsutum L.*). *Mol Biol Rep* **36**, 47–56.

Gibson, M. C. & Perrimon, N. (2003). Apicobasal polarization: epithelial form and function. *Curr Opin Cell Biol* **15**, 747–752.

Hariharan, I. K. & Bilder, D. (2006). Regulation of imaginal disc growth by tumor-suppressor genes in *Drosophila*. *Annu Rev Genet* **40**, 335–361.

Ho, C. H., Magtanong, L., Barker, S. L., Gresham, D., Nishimura, S., Natarajan, P., Koh, J. L., Porter, J., Gray, C. A. & other authors (2009). A molecular barcoded yeast ORF library enables mode-of-action analysis of bioactive compounds. *Nat Biotechnol* **27**, 369–377.

Janke, C., Magiera, M. M., Rathfelder, N., Taxis, C., Reber, S., Maekawa, H., Moreno-Borchart, A., Doenges, G., Schwob, E. & other authors (2004). A versatile toolbox for PCR-based tagging of yeast genes: new fluorescent proteins, more markers and promoter substitution cassettes. *Yeast* **21**, 947–962.

Lehman, K., Rossi, G., Adamo, J. E. & Brennwald, P. (1999). Yeast homologues of tomosyn and lethal giant larvae function in exocytosis and are associated with the plasma membrane SNARE, Sec9. *J Cell Biol* **146**, 125–140.

Levin, D. E. (2005). Cell wall integrity signaling in *Saccharomyces cerevisiae*. *Microbiol Mol Biol Rev* **69**, 262–291.

Levin, D. E. (2011). Regulation of cell wall biogenesis in *Saccharomyces cerevisiae*: the cell wall integrity signaling pathway. *Genetics* **189**, 1145–1175.

Levin, D. E. & Bartlett-Heubusch, E. (1992). Mutants in the *S. cerevisiae PKC1* gene display a cell cycle-specific osmotic stability defect. *J Cell Biol* **116**, 1221–1229.

Madden, K. & Snyder, M. (1998). Cell polarity and morphogenesis in budding yeast. *Annu Rev Microbiol* **52**, 687–744.

Pruyne, D. & Bretscher, A. (2000). Polarization of cell growth in yeast. *J Cell Sci* **113**, 571–585.

Ren, Q., Liou, L. C., Gao, Q., Bao, X. & Zhang, Z. (2012). Bir1 deletion causes malfunction of the spindle assembly checkpoint and apoptosis in yeast. *Front Oncol* **2**, 93.

Váchová, L. & Palková, Z. (2005). Physiological regulation of yeast cell death in multicellular colonies is triggered by ammonia. *J Cell Biol* **169**, 711–717.

Wach, A., Brachat, A., Pöhlmann, R. & Philippsen, P. (1994). New heterologous modules for classical or PCR-based gene disruptions in *Saccharomyces cerevisiae*. *Yeast* **10**, 1793–1808.

Yan, G., Lai, Y. & Jiang, Y. (2012). The TOR complex 1 is a direct target of Rho1 GTPase. *Mol Cell* **45**, 743–753.

Zhang, X., Wang, P., Gangar, A., Zhang, J., Brennwald, P., TerBush, D. & Guo, W. (2005). Lethal giant larvae proteins interact with the exocyst complex and are involved in polarized exocytosis. *J Cell Biol* **170**, 273–283.

Edited by: H. Sychrova